PHYSICAL REVIEW B **94**, 121401(R) (2016)

Quantum transport in the surface states of epitaxial Bi(111) thin films

Kai Zhu, Lin Wu, Xinxin Gong, Shunhao Xiao, and Xiaofeng Jin*

Department of Physics, State Key Laboratory of Surface Physics, Fudan University, Shanghai 200433, China and Collaborative Innovation Center of Advanced Microstructures, Fudan University, Shanghai 200433, China

(Received 23 February 2016; revised manuscript received 21 August 2016; published 6 September 2016)

Although bulk Bi is a prototypical semimetal with a topologically trivial electronic band structure, we show by various quantum transport measurements that epitaxial Bi(111) thin films have unexpected and nontrivial properties. Not only the top and the bottom but also the side surfaces of epitaxial Bi(111) thin films are always robustly metallic while the interior has already become insulating. We identify the coupling between the top and the bottom surface states that drives the two originally independent surface conducting channels into a single connected one. The properties of Bi(111) thin films realized could lead to promising applications in spintronics.

DOI: 10.1103/PhysRevB.94.121401

Bi is a fascinating material where many important physics phenomena were first observed. These include the de Haas–van Alphen effect [1], the quantum size effect [2], and quantum linear magnetoresistance [3], not to mention the large family of Bi-based topological insulators [4,5]. After decades of intensive theoretical and experimental investigations, many intriguing facets of the properties of Bi have been revealed. Especially, the surface properties of Bi have attracted intense attention [6]. Angle-resolved photoemission spectroscopy (ARPES) of Bi(111) shows that the Fermi surface consists of six elongated hole pockets along the $\bar{\Gamma}\bar{M}$ directions surrounding a ring-shaped electron pocket centered at $\bar{\Gamma}$, all with a two-dimensional character [7,8]. It is also demonstrated that these surface states of Bi(111) are strongly spin-orbit split with electron spin-momentum locking, and exhibit little thickness dependence for Bi(111) films on Si(111) [9–12]. Meanwhile, the quantum well states identified at the $\bar{M}$ point below the Fermi level show the characteristics of a freestanding film despite the obvious structural nonequivalence of the top and bottom surfaces [9]. It is further realized by spin-resolved ARPES that the spin polarization near the Brillouin-zone boundary is thickness dependent, presumably caused by the hybridization between the top and bottom surface states [13]. It is generally believed that these metallic surface states are rather fragile against surface adsorption or oxidation, unlike in the topological insulators [4,5]; by observing the decrease in conductivity of Bi(111) films through surface oxidization, Hirahara *et al.* declared that the Bi surface state can be destroyed by surface oxidization [14]. However, if this is true, then all the recent progress on the Bi(111) surface would not be helpful in unraveling the longstanding puzzle of why the surface or interface contribution always plays a prominent role in the electrical transport of Bi(111) film [15–17], with the consideration that Bi is not a topological insulator [18]. Therefore, whether the metallic surface states of Bi(111) are fragile or robust against surface adsorption or oxidation is a critical issue to be verified in experiment in order to reveal many of the mysterious transport properties of Bi thin films.

On the other hand, the longstanding search for the theoretically predicted semimetal-to-semiconductor (SMSC) transition in Bi films as a function of thickness has been filled with controversy [19,20]. By studying Bi(111) films epitaxially grown on BaF_2(111), Xiao *et al.* revealed that this transition does happen for Bi by reducing the film thickness to about 90 nm, but only in the film interior, while the surface remains always metallic [15]. In contrast, it was declared recently that the film interior of a 8 nm Bi(111) film is already conducting [21]. This finding, if true, excludes the possibility of an insulating phase existing in the interior of Bi(111) films below 90 nm, and reignites the controversy regarding the SMSC transition. Very recently, with high-resolution photon-energy and polarization-dependent ARPES measurements, Hirahara *et al.* confirmed that the predicted SMSC transition does happen in Bi(111) films thinner than 70 nm, but declared that the film became metallic again when the film thickness was decreased below 12 nm [22]. However, it should be noted that this finding is directly contradictory to the transport experiments in the literature, where the resistivity versus temperature curves of ultrathin Bi films always exhibit semiconducting behavior [15,17,23]. Therefore, the longstanding controversy concerning the SMSC transition in Bi(111) films is contingent upon the existence of the insulating phase, which can only be clarified by experiments.

In this Rapid Communication, we first demonstrate unambiguously that there exists a well-defined energy gap of 62 meV in the interior of a 4 nm Bi(111) film epitaxially grown on Si(111) substrate. It is important to note that the energy gap remains the same by half a monolayer (ML) of Fe deposited on the Bi(111) surface with a significant reduction of the total conductance of the system. We further observe the unanticipated Altshuler-Aronov-Spivak and Aharonov-Bohm effects in a Bi(111) nanoribbon fabricated from epitaxial films by means of photolithography and *e*-beam lithography, a fingerprint of the coherent propagation of two-dimensional electrons around the perimeter of the Bi ribbon. This result provides unequivocal evidence of the existence of robust metallic surface states not only on the top and the bottom but also on the side surfaces of the Bi(111) film. Finally, by combining the thickness-dependent conductance and weak antilocalization measurements for Bi(111) films below 15 nm, we clearly identify the electronic hybridization between the top and bottom surfaces. It is this intersurface coupling that in fact modifies the electrical conductance in a way as though it is coming from the bulk contribution in the Bi film interior. We

*Corresponding author: xfjin@fudan.edu.cn

believe that these results will help to settle some longstanding controversies about the intriguing properties of Bi, and might be useful for potential applications in future spintronic devices.

The Bi(111) films were grown by molecular beam epitaxy (MBE) on semi-insulating Si(111) substrates following the recipes adopted earlier [24]. Meanwhile, the film quality was characterized *in situ* using reflection high-energy electron diffraction (RHEED); a representative RHEED pattern is shown in the inset of Fig. 1(a), indicating the high quality of the epitaxial Bi(111) film. The films were then capped with 5 nm MgO (by direct thermal evaporation of a MgO source) on top to avoid oxidation in ambient atmosphere before being taken out of the ultrahigh vacuum for further electrical transport measurements. The transport experiments were carried out in an Oxford Cryofree magnet system with a temperature down to 1.4 K and a magnetic field up to 9 T.

Figure 1(a) plots the longitudinal square resistivity of a 4 nm Bi(111) film as a function of temperature. Note the two competing parts in the curve: one at low temperature below about 100 K showing metallic behavior ($d\rho_{xx}/dT > 0$), and the other at a higher temperature showing insulating or semiconducting behavior ($d\rho_{xx}/dT < 0$). The small upturn below 5 K in Fig. 1(a) comes from the quantum correction of the electron-electron interaction [21], and will be described in detail elsewhere. Although a curve such as this is prototypical for Bi(111) thin films in the literature [15], an apparent linear temperature dependence is directly singled out here in the experiment in a Bi thin film, as indicated by the red line in the figure. It is a strong indication that this metallic part comes from the surface or interface contribution (or both) to the total conductivity of the Bi(111) film, as it should be expected from the electron-phonon scattering for a two-dimensional metallic system, just as in a metallic surface superstructure of Ag on Si(111) [25]. Because the total conductivity in the Bi(111) film consists of the film surface as well as interior contributions, i.e., $\sigma_{xx}(T) = \sigma_{\text{interior}}(T) + \sigma_{\text{surface}}(T)$, we can then get the temperature-dependent conductivity of the film interior by $\sigma_{\text{interior}}(T) = \sigma_{xx}(T) - 1/\rho_{\text{surface}}(T)$, where $\sigma_{xx}(T) = 1/\rho_{xx}(T)$ as read out from the blue circles in the figure, while $\rho_{\text{surface}}(T) = \rho_{\text{surface}}(0) + \kappa T$ is the linear function described by the red line yet extrapolated all the way up to 300 K. In Fig. 1(b), we plot $\ln[\sigma_{\text{interior}}(T)]$ as a function of $1/T$ with the temperature range of 60–300 K, which corresponds to a change of conductivity of more than two orders of magnitude as the temperature increases from 60 to 300 K. Strikingly, this dramatically changed $\ln[\sigma_{\text{interior}}(T)]$ can be well fitted with a straight line, as shown by the red line. From the slope of the straight line we now finally obtain an electronic energy gap of 62 meV in the interior of the 4 nm Bi(111) film. This result clearly indicates that the interior of the 4 nm Bi (111) is semiconducting, therefore it is directly opposite to the claim by Hirahara *et al.* [22] that Bi(111) films become metallic again below 12 nm.

In order to verify the foregoing results, we have designed a special sample using a shadow mask technique as described elsewhere [26], i.e., a 5 nm epitaxial Bi(111) film on Si(111) with half of the surface covered *in situ* by 0.5 ML Fe before the MgO capping. In Fig. 1(c) we plot the temperature-dependent resistivity of a 5 nm Bi film with and without 0.5 ML Fe on the surface. As anticipated by the effect of magnetic impurity on the spin-momentum locking surface states [23,27–32], the total

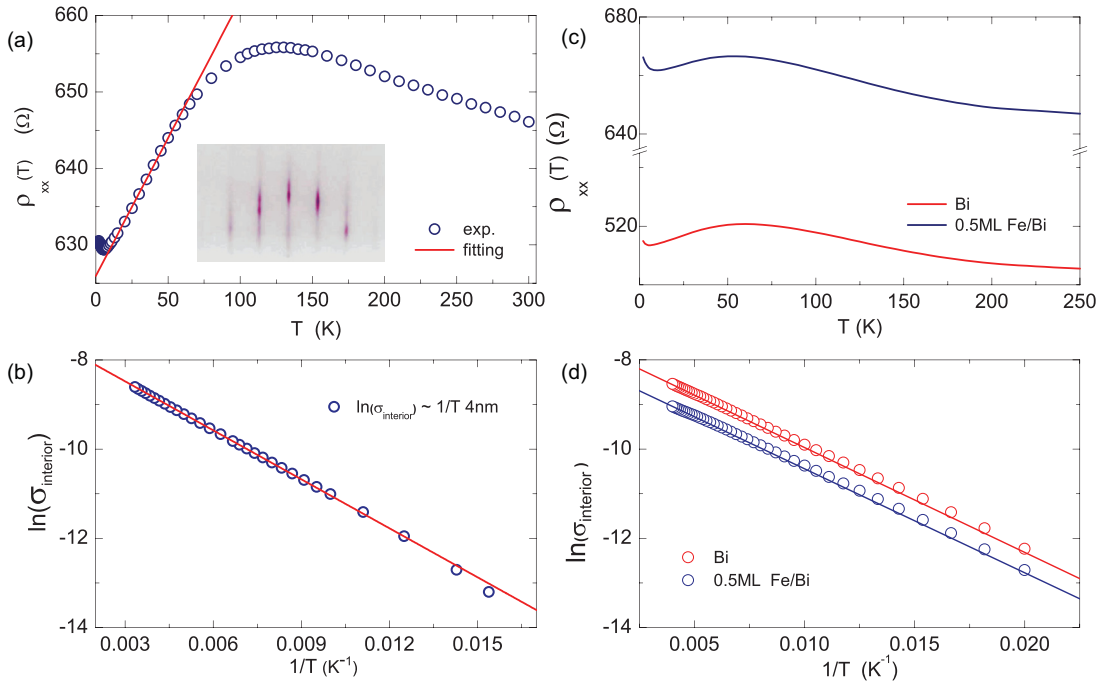

FIG. 1. (a) Temperature dependence of longitudinal square resistivity ρ_{xx} (blue circle) of a 4 nm Bi film. The red line represents the linear fitting. The inset shows a representative RHEED pattern. (b) A 62 meV gap can be extracted from the $\ln[\sigma_{\text{interior}}(T)]$ vs $1/T$ plot for the film interior. (c) The temperature-dependent resistivity of a 5 nm Bi film with and without 0.5 ML Fe surface impurities, with the procedure described in the text; the two films have the same interior gap, as indicated by the $\ln[\sigma_{\text{interior}}(T)]$ vs $1/T$ plot in (d).

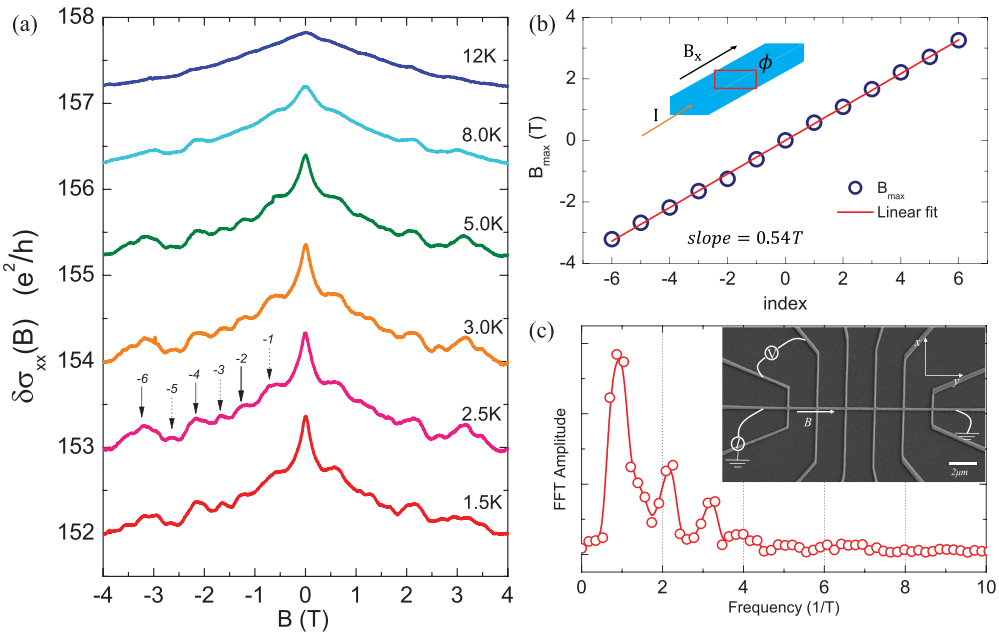

FIG. 2. (a) Magnetoconductivity measured at different temperatures with the magnetic field applied along the current direction (with a background subtraction and different curves shifted for clarity). Periodic oscillations are visible on top of a smooth background, as indicated by the arrows. (b) The field position of all periodic maxima plotted as a function of the corresponding index. (c) Fast Fourier transform of the oscillation. The inset shows the SEM picture of the device with a rectangular cross section (width $w = 220.7$ nm and thickness $d = 16.0$ nm) and the sketch for transport measurements.

conductivity is indeed significantly reduced for the sample with 0.5 ML Fe on the surface. Following a similar procedure described earlier, we plot $\ln[\sigma_{\text{interior}}(T)]$ vs $1/T$ in Fig. 1(d) for both samples with and without 0.5 ML Fe on the surface. Surprisingly, the slopes in the two cases are basically the same (an energy gap of 38 meV), which in turn provides direct evidence that the magnetic impurities on the surface of Bi(111) only affect the surface conductivity, meanwhile leaving the film interior counterpart unchanged. In addressing the second issue in the Introduction to this Rapid Communication, we conclude from these results that a Bi(111) thin film below a certain thickness does contain an insulating phase in the film interior, therefore confirming the theoretical prediction made decades ago [19,20].

Next, we demonstrate that not only the top and the bottom but also all the side surfaces of Bi(111) thin films are robustly metallic even though the film interior is insulating. It is noticed that so far all the transport experiments in the literature have indicated that the metallic surface states of Bi(111) films contribute to the total conductance, but none of them could ever state explicitly whether the contribution is only from the top or the bottom surface or from both, without mentioning that we have been totally ignorant of whether or not the side surfaces of the films are metallic. To answer this question, we have fabricated quasi-one-dimensional (1D) nanoribbons for a 16.0 nm epitaxial Bi(111) film, using a combination of photolithography and *e*-beam lithography; the inset of Fig. 2(c) shows a scanning electron microscopy(SEM) image of the device. When an external magnetic field is applied along the nanoribbon (the same direction of electrical current), quantum interference effects such as the Aharonov-Bohm effect (ABE) or the Altshuler-Aronov-Spivak effect (AAS) [33] might occur if the whole surface states of Bi(111) films are metallic yet the film interior is insulating.

Figure 2(a) plots the magnetoconductivity as a function of magnetic field at different temperatures. Pronounced and reproducible fine structures on top of a smooth background are clearly observed at lower temperatures. This feature corresponds to a periodic oscillation with an amplitude of the order of the quantized conductance (e^2/h), comparable to those observed in other quasi-1D nanostructures [34,35] and cylinders [36]. Here, as shown in Fig. 2(b), a well-defined period of 0.54 T for the oscillations is obtained by a nice linear fit between the identified conductivity maxima and the corresponding index from Fig. 2(a). If this period corresponds to the Altshuler-Aronov-Spivak effect (period of $h/2e$), then a cross-section area of 3.8×10^{-15} m^2 would be expected for the nanoribbon, which turns out to be in excellent agreement with the directly measured SEM cross-section area $S = wd = 3.5 \times 10^{-15}$ m^2. After taking the fast Fourier transform (FFT), a method commonly applied to separate the oscillatory part from the slow-varying background, a prominent peak with periodicity of h/e which corresponds to the Aharonov-Bohm effect is also resolved in Fig. 2(c). The coexistence of AAS and AB oscillations in a nanoribbon is in fact quite common in topological insulator films [35,37,38]. As expected, these oscillatory features fade away at higher temperatures, as shown in Fig. 2(a). Because the AB and AAS effects require a full revolution around the perimeter of the Bi nanoribbon for the interference, the existence of these oscillations manifests in that the metallic surface states not only exist on the top and bottom Bi(111) surfaces but also propagate coherently through the sidewalls of the ribbon. Given the fact that our nanoribbon is patterned by *e*-beam lithography, therefore all the sidewalls

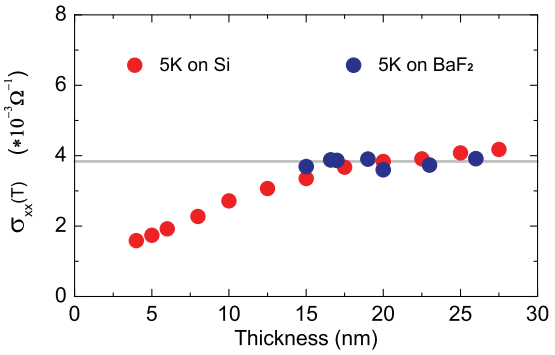

FIG. 3. Thickness dependence of surface conductivity at 5 K for Bi films on different substrates Si(111) and BaF_2(111) (from Ref. [15]).

should be terminated with dangling bonds [6] and are most likely oxidized already during the fabrication, the result also indicates that the metallic surface states of Bi(111) films are very robust, which is in strong contrast to the conclusion drawn by Hirahara *et al.* that the surface state is destroyed by oxidization [14]. It should be mentioned that similar AB and AAS oscillations were also observed in the nanowires prepared by the Ulitovsky technique, with $(10\bar{1}1)$ orientation along the wire axis [39].

Now we try to address another mysterious behavior of Bi(111) films. It was previously found in Bi(111) on BaF_2(111) that the total conductance as a function of film thickness at 5 K exhibits a kind of plateau between 15 and 25 nm (where 15 nm was the thinnest available), which is attributed to the sole contribution from the metallic surface states [15]. In contrast, it was recently observed that the conductance shows strong film thickness dependence for thinner Bi(111) films on Si(111) [21]. Obviously, these results seem to be directly contradictory. In Fig. 3, we plot the total conductance as a function of film thickness for Bi(111) films on Si(111), as shown by the red dots. Interestingly, the conductance at 5 K indeed remains almost constant between 15 and 27.5 nm, as marked by the dashed line, clearly indicating that the film interior contributes little to the conductance; this reproduces what was found previously for Bi(111) on BaF_2(111), as marked by the blue dots here [15]. On the other hand, different from the case of Bi on BaF_2(111), the epitaxial growth of Bi on Si(111) can go down to a much thinner regime, which allows us to observe the conductance decreasing for thinner films, as previously found in Ref. [21]. It can be concluded unambiguously from this result that the film interior is not metallic, otherwise the exact opposite behavior would have been observed, i.e., an increase of total conductance with decreasing film thickness because of the metallicity in the film interior, which is definitely not the case in reality. This decrease cannot be simply attributed to the surface states of Bi(111) because they remain basically unchanged in this thickness regime, as found by ARPES [10]. Instead, we believe that it is a signature of the hybridization between the top and bottom surface states. Due to the strong spin-orbit coupling in Bi, the top and bottom surface states could be visualized as two Rashba surface states with opposite spin helicity, respectively. Therefore, on either the top or bottom surface alone, the electronic scattering connecting the wave vectors of $+k$ and $-k$ is forbidden because of spin-momentum locking [40]. However, when the film thickness is reduced, the top and bottom surface states begin to hybridize, as predicted theoretically and verified by ARPES experiments [10,13,41,42]; this in turn can open up the electronic scattering channel from $+k$ on the top surface to $-k$ on the bottom surface (or vice versa), thus resulting in a decrease in the total conductance. Accordingly, instead of proving that the surface states of Bi(111) are fragile by surface oxidation, the experimental data by Hirahara *et al.* [14] could be better understood in the following way: (a) The surface oxidation on the 12 nm Bi film does produce a few layers of Bi oxide on top, thus reducing the effective thickness of the remaining Bi film underneath; it is the latter that has caused the decrease of the film conductivity, as would be exactly anticipated, as shown in Fig. 3 here. (b) For the 2.3 nm case, presumably the entire film has been oxidized, or even if only one bilayer Bi(111) was left over, the system might be driven into a two-dimensional (2D) topological insulator regime, as proposed by Murakami [43].

Finally, we show a nontrivial consequence of the hybridization of the top and bottom surface states on the coherent transport of electrons in the surface states. In Fig. 4(a) we plot a series of curves of magnetoconductivity versus temperature for a 4 nm Bi(111) film (patterned into an H-bar with a width of 200 μm by photolithography). The cusps around the zero magnetic field (perpendicular to the film plane) correspond to the typical weak antilocalization [16,44–46], which can be well described by the two-dimensional Hikami-Larkin-Nagaoka (HLN) formula

$$\Delta\sigma_{xx}(B) = \alpha\frac{e^2}{2\pi^2\hbar}\left[\Psi\left(1/2+\frac{\hbar}{4eBl_\varphi^2}\right)-\ln\left(\frac{\hbar}{4eBl_\varphi^2}\right)\right], \quad (1)$$

where e is the electronic charge, $\hbar$ is the Planck constant, l_φ is the phase coherence length, Ψ is the digamma function, and $\alpha = -1/2$, respectively [47], as shown by the black solid line for the fitting to the experimental data at 1.5 K. Figure 4(b) displays the extracted fitting results. As anticipated, the extracted phase coherence length (blue dots) decreases sensitively and monotonically from 237 nm at 2 K to 38 nm at 15 K. On the other hand, quite surprisingly, the coefficient of α (red dots) is found to be consistently close to $-1/2$ rather than -1, implying a single 2D channel, although -1 would be naively expected because of the two 2D channels of the top and the bottom surfaces.

The WAL is further investigated as a function of Bi film thickness, as shown in Fig. 4(c). Interestingly, we find the phase coherence length l_φ increases first with the film thickness, then saturates at about 320 nm. This result is consistent with the conclusion we draw from Fig. 3, that the hybridization between the top and bottom surface states in the ultrathin regime significantly activates the backscattering channel from $+k$ to $-k$. On the other hand, α is again found consistently to be around $-1/2$. Here, the real puzzle lies in why the total conductance of a Bi film is already saturated above 15 nm (negligible interaction between the top and bottom surfaces) as seen in Fig. 3, but the WAL remains as a single 2D channel (strong interaction between the top and bottom surfaces). To

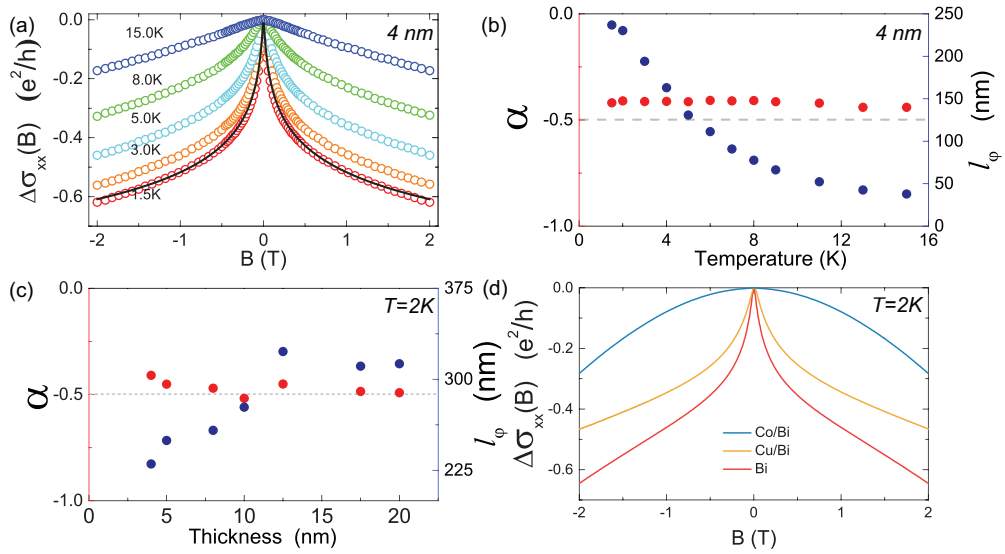

FIG. 4. Weak antilocalization in the Bi(111) films. (a) Representative magnetoconductivity curves for 4 nm Bi film with a perpendicular magnetic field at various temperatures. (b) α and l_ϕ as a function of temperature for 4 nm Bi film. (c) α and l_ϕ vs Bi film thickness at 2 K. (d) Impurity effect on weak antilocalization.

confirm that the WAL effect is very sensitive to the interaction between the top and bottom surface states, we explore the surface modification by the deposition of both magnetic (Co) and nonmagnetic (Cu) impurities (0.5 ML) on the top surface of 5 nm Bi(111) films before MgO capping, as shown in Fig. 4(d). As expected, the total conductance of these films with both Cu and Co impurities decreases as compared to that of pristine Bi thin films; meanwhile, the Cu impurity simply reduces the phase coherence length of the system from 182 to 114 nm. This is consistent with the early reports of the effect of impurities on the surface states [23,27–31]. However, it is striking to find that 0.5 ML Co on the top surface alone has completely suppressed the WAL, although the conducting 2D bottom surface states are far from directly in contact with the Co impurities. In fact, with the scenario that the top and bottom surfaces hybridize to form a single channel for electron transport, presumably the result could be understood as a consequence that the Co magnetic impurities break time-reversal symmetry of the whole system and lead to the suppression of the 2D WAL effect.

This work is supported by MOST (Grants No. 2015CB921400 and No. 2011CB921802), and NSFC (Grants No. 11374057, No. 11434003, and No. 11421404).

[1] W. J. de Haas and P. M. van Alphen, Proc. K. Ned. Akad. Wet. **33**, 1106 (1930).
[2] Y. F. Ogrin, V. N. Lutskii, and M. I. Elinson, JETP Lett. **7**, 71 (1966).
[3] A. A. Abrikosov, Europhys. Lett. **49**, 789 (2000).
[4] X.-L. Qi and S.-C. Zhang, Rev. Mod. Phys. **83**, 1057 (2011).
[5] M. Z. Hasan and C. L. Kane, Rev. Mod. Phys. **82**, 3045 (2010).
[6] P. Hofmann, Prog. Surf. Sci. **81**, 191 (2006).
[7] C. R. Ast and H. Höchst, Phys. Rev. Lett. **87**, 177602 (2001).
[8] C. R. Ast and H. Höchst, Phys. Rev. B **67**, 113102 (2003).
[9] Y. M. Koroteev, G. Bihlmayer, J. E. Gayone, E. V. Chulkov, S. Blügel, P. M. Echenique, and P. Hofmann, Phys. Rev. Lett. **93**, 046403 (2004).
[10] T. Hirahara, T. Nagao, I. Matsuda, G. Bihlmayer, E. V. Chulkov, Y. M. Koroteev, P. M. Echenique, M. Saito, and S. Hasegawa, Phys. Rev. Lett. **97**, 146803 (2006).
[11] T. Hirahara, K. Miyamoto, I. Matsuda, T. Kadono, A. Kimura, T. Nagao, G. Bihlmayer, E. V. Chulkov, S. Qiao, K. Shimada *et al.*, Phys. Rev. B **76**, 153305 (2007).
[12] A. Takayama, T. Sato, S. Souma, and T. Takahashi, Phys. Rev. Lett. **106**, 166401 (2011).
[13] A. Takayama, T. Sato, S. Souma, T. Oguchi, and T. Takahashi, Nano Lett. **12**, 1776 (2012).
[14] T. Hirahara, I. Matsuda, S. Yamazaki, N. Miyata, and S. Hasegawa, Appl. Phys. Lett. **91**, 202106 (2007).
[15] S. Xiao, D. Wei, and X. Jin, Phys. Rev. Lett. **109**, 166805 (2012).
[16] S.-L. Yin, X.-J. Liang, and H. W. Zhao, Chin. Phys. Lett. **30**, 087305 (2013).
[17] F. Pang, X.-J. Liang, Z.-L. Liao, S.-L. Yin, and D.-M. Chen, Chin. Phys. B **19**, 087201 (2010).
[18] L. Fu and C. L. Kane, Phys. Rev. B **76**, 045302 (2007).
[19] V. N. Lutskii, JETP Lett. **2**, 245 (1965).
[20] V. B. Sandomirskii, Sov. Phys. JETP **25**, 202 (1967).
[21] M. Aitani, T. Hirahara, S. Ichinokura, M. Hanaduka, D. Shin, and S. Hasegawa, Phys. Rev. Lett. **113**, 206802 (2014).
[22] T. Hirahara, T. Shirai, T. Hajiri, M. Matsunami, K. Tanaka, S. Kimura, S. Hasegawa, and K. Kobayashi, Phys. Rev. Lett. **115**, 106803 (2015).
[23] D. Lükermann, S. Sologub, H. Pfnür, C. Klein, M. Horn-von Hoegen, and C. Tegenkamp, Materialwiss. Werkstofftech. **44**, 210 (2013).

[24] T. Nagao, J. T. Sadowski, M. Saito, S. Yaginuma, Y. Fujikawa, T. Kogure, T. Ohno, Y. Hasegawa, S. Hasegawa, and T. Sakurai, Phys. Rev. Lett. **93**, 105501 (2004).

[25] I. Matsuda, C. Liu, T. Hirahara, M. Ueno, T. Tanikawa, T. Kanagawa, R. Hobara, S. Yamazaki, S. Hasegawa, and K. Kobayashi, Phys. Rev. Lett. **99**, 146805 (2007).

[26] J. Xu, L. Wu, Y. Li, D. Tian, K. Zhu, X. Gong, and X. Jin, Sci. Bull. **60**, 1261 (2015).

[27] D. Lükermann, S. Sologub, H. Pfnür, and C. Tegenkamp, Phys. Rev. B **83**, 245425 (2011).

[28] D. Lükermann, S. Sologub, H. Pfnür, C. Klein, M. Horn-von Hoegen, and C. Tegenkamp, Phys. Rev. B **86**, 195432 (2012).

[29] K. Zhu, L. Wu, X. Gong, S. Xiao, X. Jin *et al.*, arXiv:1403.0066.

[30] P. Kröger, S. Sologub, C. Tegenkamp, and H. Pfnür, J. Phys.: Condens. Matter **26**, 225002 (2014).

[31] C. Klein, N. J. Vollmers, U. Gerstmann, P. Zahl, D. Lükermann, G. Jnawali, H. Pfnür, C. Tegenkamp, P. Sutter, W. G. Schmidt *et al.*, Phys. Rev. B **91**, 195441 (2015).

[32] H.-T. He, G. Wang, T. Zhang, I.-K. Sou, G. K. L. Wong, J.-N. Wang, H.-Z. Lu, S.-Q. Shen, and F.-C. Zhang, Phys. Rev. Lett. **106**, 166805 (2011).

[33] B. L. Altshuler, A. G. Aronov, and B. Z. Spivak, JETP Lett. **33**, 94 (1981).

[34] T. E. Huber, K. Celestine, and M. J. Graf, Phys. Rev. B **67**, 245317 (2003).

[35] H. Peng, K. Lai, D. Kong, S. Meister, Y. Chen, X.-L. Qi, S.-C. Zhang, Z.-X. Shen, and Y. Cui, Nat. Mater. **9**, 225 (2010).

[36] A. G. Aronov and Y. V. Sharvin, Rev. Mod. Phys. **59**, 755 (1987).

[37] F. Xiu, L. He, Y. Wang, L. Cheng, L.-T. Chang, M. Lang, G. Huang, X. Kou, Y. Zhou, X. Jiang *et al.*, Nat. Nanotechnol. **6**, 216 (2011).

[38] J. Dufouleur, L. Veyrat, A. Teichgräber, S. Neuhaus, C. Nowka, S. Hampel, J. Cayssol, J. Schumann, B. Eichler, O. G. Schmidt *et al.*, Phys. Rev. Lett. **110**, 186806 (2013).

[39] L. Konopko, T. E. Huber, and A. Nikolaeva, J. Low Temp. Phys. **159**, 253 (2009).

[40] M. C. Cottin, C. A. Bobisch, J. Schaffert, G. Jnawali, A. Sonntag, G. Bihlmayer, and R. Möller, Appl. Phys. Lett. **98**, 022108 (2011).

[41] Y. M. Koroteev, G. Bihlmayer, E. V. Chulkov, and S. Blügel, Phys. Rev. B **77**, 045428 (2008).

[42] T. Hirahara, K. Miyamoto, A. Kimura, Y. Niinuma, G. Bihlmayer, E. V. Chulkov, T. Nagao, I. Matsuda, S. Qiao, K. Shimada *et al.*, New J. Phys. **10**, 083038 (2008).

[43] S. Murakami, Phys. Rev. Lett. **97**, 236805 (2006).

[44] G. Bergmann, Phys. Rep. **107**, 1 (1984).

[45] Y. F. Komnik, E. I. Bukhshtab, V. V. Andrievskii, and A. V. Butenko, J. Low Temp. Phys. **52**, 315 (1983).

[46] S. Sangiao, N. Marcano, J. Fan, L. Morellon, M. R. Ibarra, and J. M. D. Teresa, Europhys. Lett. **95**, 37002 (2011).

[47] S. Hikami, A. I. Larkin, and Y. Nagaoka, Prog. Theor. Phys. **63**, 707 (1980).